Dyes and Pigments 117 (2015) 37–48

Contents lists available at ScienceDirect

Dyes and Pigments

journal homepage: www.elsevier.com/locate/dyepig

The nature of thermochromic effects in dyeings with indigo, 6-bromoindigo, and 6,6′-dibromoindigo, components of Tyrian purple

Keith Ramig [a, *], Olga Lavinda [a, 1], David J. Szalda [a], Irina Mironova [a, 2], Sasan Karimi [b], Federica Pozzi [c, 3], Nilam Shah [d], Jacopo Samson [e], Hiroko Ajiki [e, 4], Lou Massa [f], Dimitrios Mantzouris [g], Ioannis Karapanagiotis [h], Christopher Cooksey [i]

[a] Department of Natural Sciences, Box A0506, Baruch College of the City University of New York, 1 Bernard Baruch Way, New York, NY 10010, USA
[b] Department of Chemistry, Queensborough Community College of the City University of New York, 222-05 56th Ave., Bayside, NY 11364, USA
[c] Department of Conservation, Art Institute of Chicago, 111 South Michigan Ave., Chicago, IL 60603, USA
[d] Department of Chemistry, Northwestern University, 2145 Sheridan Road, Evanston, IL 60208, USA
[e] Department of Chemistry and Biochemistry, Hunter College and the Graduate School, City University of New York, 695 Park Ave., New York, NY 10065, USA
[f] Departments of Chemistry & Physics, Hunter College and the Graduate School, City University of New York, 695 Park Ave., New York, NY 10065, USA
[g] Ormylia Foundation, Art Diagnosis Center, Ormylia 63071, Greece
[h] University Ecclesiastical Academy of Thessaloniki, Thessaloniki 54250, Greece
[i] 59 Swiss Avenue, Watford, Hertfordshire, WD18 7LL, England, UK

ARTICLE INFO

Article history:
Received 2 December 2014
Received in revised form
24 January 2015
Accepted 27 January 2015
Available online 7 February 2015

This article is dedicated to Professor Theodore Cohen of the University of Pittsburgh, on the occasion of his 85th birthday.

Keywords:
Indigo
6-Bromoindigo
6,6′-Dibromoindigo
Tyrian purple
Thermochromic
Nanotube

ABSTRACT

Thirteen fabrics are each dyed with either indigo, or 6-bromoindigo, or 6,6′-dibromoindigo. When the dyed fabrics, which had not undergone any finishing procedures, are boiled in water for 10 min, color changes are observed: many indigo- and 6-bromoindigo-dyed fabrics turn more blue, while many 6,6′-dibromoindigo-dyed fabrics turn more red. These color changes are characterized by reflectance spectra and colorimetry data. Evidence is presented that the color changes are related to particle sizes of the dyes: 6,6′-dibromoindigo-dyed carbon nanotubes, used as a fabric surrogate, show an increase in dye-particle size upon heating, as judged by electron microscopy. Because we have shown previously that 6-bromoindigo-dyed carbon nanotubes give decreased dye-particle size when heated, we infer that, no matter the indigoid or fabric, smaller particles tend to cause a bluer fabric shade, while larger particles cause a redder shade.

1. Introduction

The subject of Tyrian purple has provoked much interest for a very long time. The manufacture of purple dyed textiles from shellfish grew to be a major industry starting in Crete in the Mediterranean Sea about 1800 BC. The industry grew all around the Mediterranean and then contracted, being finally extinguished when the last of the imperial dyeworks at Constantinople (now Istanbul) was destroyed by Sultan Mehmet II in 1453. But, the purple was not a European monopoly. It is found wherever there are shellfish, notably Central America and Japan [1]. Of the various descriptions of purple dyeing in the ancient world, the most complete and best known is that of Pliny the Elder [2]. A modern successful reconstruction of the dyeing process found that his ten-day reduction time could be decreased to three to five days [3]. The social significance of the purple has been explored [4].

* Corresponding author. Tel.: +1 646 660 6243; fax: +1 646 660 6201.
E-mail address: keith.ramig@baruch.cuny.edu (K. Ramig).
[1] Current address: Department of Chemistry, New York University, 100 Washington Square East, New York, NY 10003, USA.
[2] Current address: 24 University Manor East, Hershey, PA 17033, USA.
[3] Current address: Department of Conservation, Solomon R. Guggenheim Museum, 1071 5th Ave., New York, NY 10128, USA.
[4] Current address: Department of Chemistry, Queens College of the City University of New York, 65-30 Kissena Blvd, Flushing, NY 11367, USA.

http://dx.doi.org/10.1016/j.dyepig.2015.01.025
0143-7208/

Over the years, many investigations of the dye and its color variations have been reported. In the 19th century, before the chemistry of the purple production was understood, Edward Schunck studied the English mollusk, the dog whelk [5]. The major component of Tyrian purple, 6,6′-dibromoindigo (DBI), was only identified in the early 20th century by Paul Friedländer after heroic efforts involving 12,000 *Murex brandaris* mollusks [6]. It has long been known that some mollusks, especially *Murex trunculus*, produce a more blue color [7], and this was usually assumed to be due to indigo. But it might have been due to 6-bromoindigo (MBI). However, this new component was not detected until an HPLC method became available [8]. A more blue shade can be obtained if the reduced form of DBI, l*euco*-DBI, is exposed to sunlight whereupon it is debrominated. Then on oxidation, MBI and indigo are formed. So the color obtained depends not only on the mollusk used but also on how it is processed. In addition, the substrate has a large influence on the shade obtained when dyeing textiles with *leuco*-DBI [9].

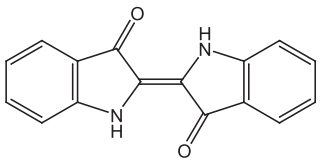

Indigo

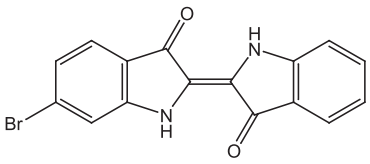

6-Bromoindigo

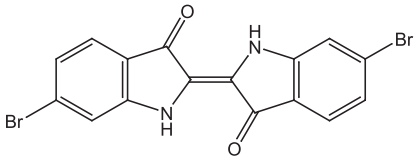

6,6'-Dibromoindigo

In a recent article we reported a study of the thermochromic properties of fabrics dyed with indigo, MBI, and DBI [10]. We showed that, while some indigo-dyed fabrics give slight color changes upon heating in water, color changes of MBI- and DBI-dyed fabrics can be more pronounced. Most interesting was the finding that many indigo- and MBI-dyed fabrics after heating give color changes toward longer reflected wavelengths of light, while the heat-induced color changes of DBI-dyed fabrics are toward shorter reflected wavelengths. Many of the MBI- and DBI-dyed fabrics show reflectance minima with a shoulder (defined as a bulge in the curve on either side of the minimum), one around 530 nm and the other around 610 nm; it is the relative intensities of the minimum and shoulder that determine a particular fabric's color – purple, violet, or blue. These spectral features indicate presence of two types of dye aggregates, one giving a more reddish color, while the other, more bluish. In light of Cooksey and Sinclair's earlier dilution studies which showed that small dye aggregates on fabric appear more blue [9], we hypothesized that the heat-induced color changes may have the same basis. To prepare a dyed-fabric surrogate amenable to electron microscopic analysis, we deposited MBI dye aggregates on carbon nanotubes. The nanotubes showed nanometrically sized dye aggregates, which became significantly smaller after boiling in water for a short time. Thus, either dilution of the dye vat or heating of the dyed fabric in water produces smaller dye aggregates which give a bluer fabric.

This article extends the findings of our previous study mentioned above, resulting in an explanation of the thermochromic effects seen in dyeings with all three indigoids. We will first present X-ray crystallographic data that indicate the thermochromic behavior of MBI-dyed fabrics is particular to dye aggregates on fabric, and is not a property of the bulk dye. To rule out the possibility of a chemical reaction causing the observed color changes, we present HPLC data of extracts from the fabrics that show no significant chemical degradation of the dye. Then it will be seen that the divergent thermochromic behavior of DBI-dyed fabrics vs. that of indigo- and MBI-dyed fabrics, is not limited to wool and silk, which were the subjects of our earlier study. A wide variety of synthetic fabrics also exhibit this behavior, as will be shown by reflectance spectral and colorimetric analyses. Finally, we will show that DBI-dyed carbon nanotubes contain dye aggregates that become larger upon boiling in water, which is the opposite behavior of MBI-dyed nanotubes.

2. Materials and methods

2.1. Chemicals and materials

The 13 fabrics used in the dyeing were obtained as multi-fabric strips (style # 43) from Testfabrics, Inc. There were three natural fibers: wool, cotton, and silk; three cotton-based synthetics: filament acetate (diacetate), filament triacetate, and viscose (Rayon); three polyacrylics: SEF (modacrylic), Creslan 61, and Orlon 75; two polyesters: Dacron 54 and Dacron 64; Nylon 66; and polypropylene. Single-walled carbon nanotubes (40–60 wt % carbon basis, D x L 2–10 nm x 1–5 μm, bundle dimensions), tetrahydrofuran (≥99.9%, inhibitor-free), sodium hydrosulfite (sodium dithionite; technical grade, 85%), DMSO (HPLC-grade), and indigo (95%) were obtained from Sigma–Aldrich. Ethyl benzoate (99%) was obtained from Alfa Aesar. Water (HPLC-grade) was obtained from Chem-Lab. Acetonitrile (HPLC-grade) was obtained from J. T. Baker. Trifluoroacetic acid (HPLC-grade) was obtained from Riedel-de Haën.

2.2. Instrumentation and analysis methods

2.2.1. X-ray crystallographic analysis

Crystallographic information was obtained using a Bruker Kappa APEX II diffractometer equipped with an Oxford Cryostream Cooler.

2.2.2. Visible reflectance spectra

Visible reflectance spectra of the first-pass dyeings were obtained in dual-beam mode using a Varian Cary 50 Bio UV–Vis spectrophotometer equipped with a Barrelino remote diffuse reflection probe by Harrick Scientific and a xenon flash lamp. The scan range was 200–800 nm with a maximum scan rate of 120 nm/s. Spectra of undyed fabrics were taken before each measurement and used as a calibration reference. The data were processed using Cary WinUV and Origin software applications.

Visible reflectance spectra of the second-pass dyeings were obtained using a Varian Cary 5000 UV–Vis–NIR spectrophotometer equipped with an internal diffuse reflectance accessory that consists of a 110-mm-diameter integrating sphere. The scan range was 350–800 nm with a scan rate of 600 nm/min. Reflectance measurements of fabric samples were made relative to a polytetrafluoroethylene standard.

2.2.3. Colorimetric analysis

CIELAB data were collected with a Konica Minolta Color Reader CR-10 tristimulus colorimeter, with a 10-mm/8-mm aperture/viewing area, 8° illumination angle with CIE standard illuminant D_{65}, CIE 10° viewing angle with diffuse viewing. All samples were backed with an opaque white background. For the fabrics of the multi-fabric strips, the aperture was too large and was modified by use of an opaque white mask with a 4 × 4 mm aperture. This modified aperture was tested on several larger dyed fabrics, and the colorimetric data obtained had higher L^* values, and lower a^* and b^* values, than data obtained with the unmodified aperture. But the relative magnitudes of, and differences in, the values obtained with the modified aperture were still found to be valid in drawing conclusions about color differences between two fabrics. The values of the larger fabric samples obtained with the unmodified aperture were the averages of at least five measurements taken from different spots on the fabrics; standard deviations were small, and are listed along with the raw data in the Supplementary Data section (see Table S2). For the multi-fabric strips using the modified aperture, there are no standard deviations since only one measurement was taken for each fabric; however, a standard deviation of 0.8 can be assumed for the L^* values, while 0.4 can be assumed for the a^* and b^* values, based on the averages of the standard deviations seen in measurements of the silk- and wool-alone dyeings.

2.2.4. HPLC analysis

The HPLC-DAD system (Thermoquest) consisted of a model 4000 quaternary HPLC pump, an SCM 3000 vacuum degasser, an AS3000 auto sampler with column oven, a Rheodyne 7725i injector with 20-μL sample loop and a diode array detector UV 6000LP. Analyses were carried out with an Alltima HP C18 column (Alltech; 5 μm particle size, i.d. 250 mm × 3.0 mm) at a stable temperature of 35 °C. The gradient elution program utilized two solvents: solvent A: H_2O—0.1% trifluoroacetic acid and solvent B: acetonitrile—0.1% trifluoroacetic acid [11]. A detector wavelength of 288 nm was used for peak area integrations.

A method devised and evaluated previously [11] for the extraction of Tyrian purple was applied to extract the colorants from the fabrics: Around 5 mg of the dyed fabric was weighed precisely. The sample was cut into minute pieces, forming a homogeneous powder. This was transferred to a closed vial containing 200 μL DMSO. The vial was placed in an ultrasonic bath for 30 s, and then was heated at 80 °C for 10 min. After centrifugation, the supernatant liquid was analyzed by HPLC.

HPLC analyses of the dyed wool and silk were carried out in triplicate and mean values of the HPLC integrated areas were calculated for the detected compounds. These were normalized taking into account the masses of the fabric samples. Relative standard deviations were calculated (see Table S4 in the Supplementary Data section).

2.2.5. TEM analysis

Transmission electron microscopy (TEM) data were collected at 200 kV with a Jeol 2100 instrument equipped with an EDAX energy dispersive X-ray spectrometer. All data were collected at the eucentric height to ensure reproducibility of measurements.

The dry powder of DBI-dyed single-wall carbon nanotubes was crushed on a cleaned glass slide using weighing paper. The mixture was then dispersed onto the cleaned, curved portion of a pipette bulb by gently rolling the bulb across the mixture on the glass slide. The bulb was then rolled, in one pass, across a lacey-carbon coated copper TEM grid. The "dry" delivery was chosen to rule out any possible artifacts due to residual solvent upon imaging. In order to rule out the lacey carbon artifact (i.e. single carbon nanotubes and lacey carbon both have filamentous morphologies), images were taken in between the openings of the lacey carbon.

Average particle sizes were determined by manually averaging the sizes of 50 particles from the TEM micrographs (see Figures S28 and S29 in the Supplementary Data section) using ImageJ software. The manual counting method was found to be highly accurate because when images with higher magnification are zoomed in, the pixelated edges can be well distinguished and errors in size determination are minimized. Also, the size histogram displays the average sizes of many particles therefore the errors in size measurement are further minimized.

2.3. Preparation of dyes

DBI was synthesized by the procedure of Tanoue et al. [12]. Purity was established by NMR and TLC analysis of the *N*, *N*′-bis(-trifluoroacetyl) derivative [13,14], and by HPLC [15].

MBI was prepared by the procedure of Clark and Cooksey [13]. While their reported yield of MBI is 20%, in our hands the reaction produces consistently a yield in the 40% range. The reason for this discrepancy is unclear, as the literature procedure was followed to the letter. However, some of the recrystallization parameters are unspecified, so we present here our recrystallization procedure from a reaction that was performed on the same scale as Clark and Cooksey's. From a procedure that used 4.2 mmol of acetoxyindole (the limiting reagent), 790 mg (55% crude yield) of crude MBI as a violet solid was obtained. (Clark and Cooksey report the color as dark blue.) This was dissolved in ethyl benzoate (100 μL) under N_2, and the mixture was heated at reflux for 30 min. The mixture was allowed to cool to r. t., and suction filtered. Isolated was 590 mg (41% yield) of product as a dark-violet powder. (Clark and Cooksey report the color as black with a coppery lustre.) We have repeated this procedure at double the scale, and the percent yields are within two percent of the values above. Purity was established by NMR analysis of the *N*, *N*′-bis(trifluoroacetyl) derivative [13,14], and by HPLC [15].

2.4. Crystallization and sublimation techniques

2.4.1. Production of MBI crystals amenable to X-ray crystallographic analysis: by recrystallization

A 250-μL 3-neck round-bottom flask fitted with a water condenser was swept with N_2, and kept under a positive pressure of N_2 during the recrystallization. A mixture of MBI (300 mg) and ethyl benzoate (50 μL) was introduced, and heated at reflux (212 °C) with magnetic stirring for 30 min. The dark-violet mixture was allowed to cool to 205 °C at a rate of 1–2 °C/h, at which time stirring was discontinued. Within a few hours, shiny dark-violet crystalline particles began to form. The temperature was kept at 205 °C overnight, after which time the mixture was allowed to cool to r. t. The mixture was suction filtered, washing with ethanol. Isolated was 256 mg of two types of crystals, the forms of which are easily discerned at a magnification of 10×. The large crystals are the majority; these are opaque, in the form of rectangular prisms, approximately 0.5 × 0.1 × < 0.05 mm in size, and dark-violet with a metallic sheen. A minority (≤10%) of the crystals are in the form of slightly smaller, much thinner rectangular prisms, are blue in color, and translucent. The large opaque crystals were selected for our previous single-crystal X-ray determination [16], while the smaller translucent crystals were too small and fragile for this. Ziderman has previously noted the appearance of MBI crystals of two different colors [17].

2.4.2. Macro-scale sublimation and vapor deposition of MBI

MBI (50 mg) was placed in a standard glass laboratory vacuum-sublimation apparatus (20 cm height x 6 cm i.d.; obtained from Ace Glass Inc.), and a pressure of 5 mm Hg was attained before heating. The coolant was dry ice. Vapor deposition began to occur at 190 °C and continued to 300 °C, during which time the heated crystals vibrated and moved about quite markedly. The MBI was deposited as a blue powder. No distinguishable crystalline features could be seen at a magnification of 40×. No further analysis was performed.

2.4.3. Production of MBI crystals amenable to X-ray crystallographic analysis: by semi-micro-scale sublimation and vapor deposition

A much smaller apparatus than above was fabricated from a 9 x 80-mm test tube, into which a dry-ice cooled finger (6-mm o.d. glass tubing flame-sealed shut on the bottom) was lowered. The separation between the bottoms of the outer and inner tubes was approximately 4 mm. MBI (20 mg) was placed in the bottom of the outer tube and heat was applied to achieve sublimation. A reddish gas initially formed, and deposited on the inner tube as a crystalline solid. These crystals were the same color (dark-violet) as those obtained from recrystallization, but were different in form, being more like flattened blunt rectangular needles. These were subjected to X-ray analysis (see Section 3.1 and Table 1 below).

2.4.4. Micro-scale sublimation and vapor deposition of MBI

A small amount of MBI was placed in the bottom of a melting-point capillary, and heated with a heat gun until a red-purple gas was produced. This gas crystallized on the cooler part of the capillary as dark-violet rectangular prisms, apparently identical to the opaque crystals obtained above from solvent. These were not analyzed further. A video of this experiment can be viewed at: https://www.youtube.com/watch?v=3oNw-khx30E.

2.5. Dyeing procedures

2.5.1. Dyeing of multi-fabric strips

The multi-fabric strips, silk, and wool were dyed by the procedure we reported [10], a variation of Cooksey and Sinclair's earlier procedure [9]. A standard dye concentration was set at 0.036 mmol indigoid/gram of fabric.

2.5.2. Dyeing of wool alone

The wool described in Section 3.2. was dyed by the standard procedure for all three dyes. The detailed procedure for DBI-dyed wool: A 250-μL 3-neck round-bottom flask fitted with a water condenser was swept with N_2, and kept under a positive pressure of N_2 during the dyeing. Distilled water (100 μL) and THF (15 μL) were introduced, followed by NaOH (0.50 g, 13 mmol). The solution was brought to reflux (75–80 °C) with magnetic stirring, and $Na_2S_2O_4$ (0.50 g, 85% purity, 2.4 mmol) was added, followed immediately by DBI (21 mg, 0.050 mmol), which had been finely ground in an agate mortar. At this point, the room lights were turned off and the flask was wrapped in aluminum foil. A yellow-green solution was obtained after 15 min at reflux. Addition of NH_4Cl (2.0 g, 37 mmol) gave the *leuco* form of the dye, used to dye both fabric and nanotubes; nanotube dyeing is described below. Wool fabric (1.4 g), which had been soaked in dilute soap solution, was introduced. The stirring rate was reduced, and the solution was heated at reflux for 15 min. The fabric was removed from the flask and exposed to air, while still protected from light. After at least 30 min of air exposure, the fabric was rinsed in aqueous 1% aqueous HOAc solution and allowed to dry. Second and third passes were made in the same manner with additional fabric. The dyeings were analyzed without any further finishing procedures.

2.5.3. Dyeing of nanotubes

A 1-dram vial was purged with N_2, and carbon nanotubes (30 mg) were introduced. The vial was placed in a water bath at 50 ± 2 °C, and a solution (2 μL) containing the *leuco* form of DBI, prepared as above, was added. After 15 min of stirring under N_2, the black suspension was suction filtered, washing with 3 portions of distilled water. After 30 min of suction, the black powder was washed with 1 μL 1% HOAc solution. The filtrates were all clear and colorless. After 30 min of air-drying, 30 mg of black powder was isolated.

3. Results and discussion

3.1. Form and color variations in MBI crystals

Ziderman has found that wool dyed with MBI turns from its original violet color to blue rapidly upon immersion in water and heating to 60 °C, and has reported that MBI itself changes color from violet to blue after sublimation and vapor deposition [17]. Ziderman also notes the same color change upon simple heating of MBI [18]. We have found that MBI crystals do not give a color change upon heating to 200 °C, at which point sublimation begins [10]. We will show below that a blue form of MBI can result from sublimation/vapor deposition of crystals originally dark-violet in color, and that this color change is highly dependent on the dimensions of the sublimation apparatus.

We have reported the single-crystal X-ray determination of MBI's molecular structure [16]. The crystals used in that study were obtained by recrystallization from ethyl benzoate, as described in Section 2.4.1. We also tried to obtain suitable crystals by vacuum sublimation/vapor deposition using standard-sized apparatus (see Section 2.4.2), but the crystals are much too small, occurring as a powder. However, we note that this powder is indeed blue in color. If a small test tube is used as apparatus for sublimation at atmospheric pressure (see Section 2.4.3), then the deposited crystals are identical in color but different in form, compared to those obtained from recrystallization. These crystals obtained by the method of Section 2.4.3. are too small for a full single-crystal study, but large enough to determine the cell constants (see Table 1). Finally, if the sublimation/vapor deposition occurs inside a melting-point capillary (see Section 2.4.4), then the deposited crystals are identical in form and color to those obtained by recrystallization.

The data above show that both the color and form of vapor-deposited MBI are highly dependent on the dimensions of the sublimation apparatus employed. When the dimensions are large, the resulting MBI is in the form of a blue powder. This may be the

Table 1
Single-crystal X-ray data of MBI obtained by recrystallization and vapor deposition, at various temperatures.

Entry	Method	T (°C)	a	b	c	β	Volume	# reflec.	θ min	θ max
1	recrys.	−100	12.346(3)	4.6558(12)	11.607(3)	105.856(8)	641.82	1383	3.58	25.46
2	subl.	−100	12.411(7)	4.713(3)	11.713(7)	105.89(3)	659.45	391	3.41	25.86
3	recrys.	22	12.3047(10)	4.6905(4)	11.7444(10)	105.636(4)	652.75	751	3.44	17.28
4	recrys.	77	12.365(4)	4.7042(17)	11.810(4)	105.005(11)	663.57	789	3.41	17.49

form that Ziderman saw in his study [17]. When the sublimation apparatus is a small test tube, the crystals are dark-violet in color, but are visibly different in form from those obtained by recrystallization. However, crystals obtained by sublimation in the test tube are crystallographically identical to those obtained from recrystallization, according to the cell constants listed in Table 1.

Table 1 reveals selected crystal parameters of crystals at three different temperatures. Entry 1 shows data from our recent publication [16]. The crystal was obtained by the method of Section 2.4.1, recrystallization. Entry 2 shows that a vapor-deposited crystal obtained by the method of Section 2.4.3 has nearly identical crystal parameters to those from entry 1, despite being different in visible form. The crystal grown by vapor deposition was much smaller and therefore diffracted X-rays weakly as can be seen by the decrease in the number of reflections used to determine the cell constants. Determinations of the crystal from entry 1 at elevated temperatures of 22 °C and 77 °C (entries 3 and 4) show little or no change, other than the expected increases in cell volume and length of the cell axis. No change in the color of the crystal could be observed upon heating. The highest temperature at which the cell could be reasonably determined was 77 °C, because as the temperature increased the intensity of the reflections decreased. No change in the molecular structure of MBI could be observed but all the refinements except the one of entry 1 which we have reported previously [16] were of poor quality because of the small number of reflections with $I > 2\sigma(I)$ (see Table S3 in the Supplementary Data section for additional data and discussion). The determination at 77 °C indicates that, at a temperature which causes rapid color change of MBI-dyed wool in water, there is no significant change in the crystal structure of the bulk dye molecule. Since MBI unadsorbed on fabric does not change color at this temperature, the thermochromic effect of the dye is due to its adsorption on fabric, and is not a property of the bulk dye.

3.2. Reflectance and colorimetric analysis of fabrics dyed with indigo, MBI, and DBI: the thermochromic effects

3.2.1. Reflectance spectral analysis of dyed fabrics

Fig. 1 shows three multi-fabric strips dyed with either indigo, MBI, or DBI, according to the procedure from our earlier article [10]. The dyeings were analyzed in crude form, with no after-treatment of any kind. The vats from both the MBI and DBI dyeings were exhausted after three passes, while with indigo, a fourth pass gave a dyed strip that still was highly colored. With some fabrics, MBI and DBI dyeings become more blue after each pass, which has been noted and explained by Clark and Cooksey [13] as being due to diminishment of dye particle-size.

The general trends in colors seen are that indigo dyes fabrics blue-green to blue, MBI dyes blue-violet to violet, and DBI dyes blue-violet to purple. The shades of indigo dyeings vary less between fabrics than the shades of MBI and DBI dyeings. Several of the fabrics from the MBI dyeing appear black to the eye; this means that the *leuco* or colorless reduced form of the dye, which permeates the fabric before aerial oxidation reveals the color, is very strongly attracted to the fabric. Simply boiling the strip in water for 10 min causes marked color changes for many of the fabrics (see Figure S26 in the Supplementary Data section). Fig. 2 shows the reflectance spectra of wool from the multi-fabric strips of Fig. 1. These three spectra typify the behavior of the other dyed fabrics, where the heated and unheated curves either nearly coincide with each other, as in Fig. 2a, or differ markedly, as in Fig. 2b and c. (The spectra of the rest of the fabrics can be found in Figures S1–S25 in the Supplementary Data section.) The shoulders indicated in Fig. 2b and c are considered to be peaks of lesser intensity, which merge with the main peaks. Thus, the shoulders can be visually extrapolated to give secondary peaks, with approximate minima (λ_{min}, in Fig. 2) of their own. Heating of the fabric can cause the main minimum to disappear, as in MBI-dyed wool, or can cause the shoulder to disappear, as in DBI-dyed wool.

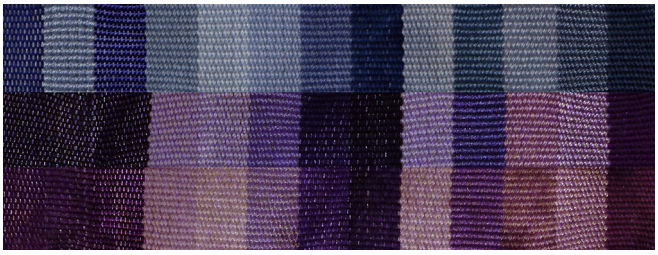

Fig. 1. First passes of multi-fabric strips dyed with indigoids; top to bottom: indigo, MBI, DBI. Fabrics, l to r: filament acetate (diacetate), SEF (modacrylic), filament triacetate, bleached cotton, Creslan 61, Dacron 54, Dacron 64, Nylon 66, Orlon 75, spun silk, polypropylene, viscose (Rayon), worsted wool.

Table 2 shows a summary of features seen in the reflectance spectra of all the dyed fabrics. The reflectance λ_{min} values of the unheated samples vary from 530 to 660 nm. For some of the indigo- and MBI-dyed fabrics, and for almost all of the DBI-dyed fabrics, λ_{min} of the main peak does not give a good idea of what the perceived colors are. To give a more accurate representation of color, two wavelength values for many fabrics should be tabulated, one for the minimum and one for the shoulder; this is the case in particular for DBI-dyed fabrics, which show shouldered peaks in almost every case. Other studies have noted that brominated indigoid dyeings can give reflectance spectra with shouldered minima [9,10,13,15].

Dramatic irreversible color changes are seen in many of the dyed fabrics simply upon boiling in water for 10 min (see Figure S26 in the Supplementary Data section). The color changes in the majority of cases are not due solely to shifts in the positions of the λ_{min} values, but are in many cases due to the shouldering effects mentioned above, leading to either a marked bluing or reddening of the fabrics. DBI-dyed fabrics show the most and strongest thermochromic effects, and result in reddening where there is this effect. Indigo- and MBI-dyed fabrics on the other hand, give only bluing or graying when the thermochromic effect obtains.

The same analysis was applied to the second-pass dyeings, to determine the effect of dilution. Also, data for the second-pass dyeings was collected because in some of the first-pass dyeings, the dye was too concentrated to give meaningful reflectance curves, i.e. the peaks were too broad to show any features. So, where indicated in Table 2, the second-pass data was substituted for first-pass data. The pictures and reflectance data of the second-pass dyeings (see Figure S26 and Table S1 in the Supplementary Data section) show that the thermochromic effect is just as prevalent as in the first-pass dyeings.

At similar concentrations of dye, DBI-dyed wool looks very similar to MBI-dyed wool, and their reflectance spectra are nearly indistinguishable; both exhibit minima at lower wavelengths, and have shoulders at higher wavelengths. We and others have demonstrated this previously [9,10,13]. In contrast, indigo-dyed wool shows no shoulder on its minimum in the blue-green region of the reflectance spectrum. The reflectance minimum of indigo-dyed wool is very near the wavelength of the shoulders of both MBI- and DBI-dyed wool (see Fig. 2). The similarities in spectra of indigoid-dyed wool have led to some confusion in the literature. Koren's recent study [15] gives a detailed analysis of the reflectance spectra of multi-fabric strips dyed with indigo, MBI, and DBI. The reflectance spectra in many cases show that brominated indigoid dyeings do give peaks with shoulders, including MBI-dyed wool,

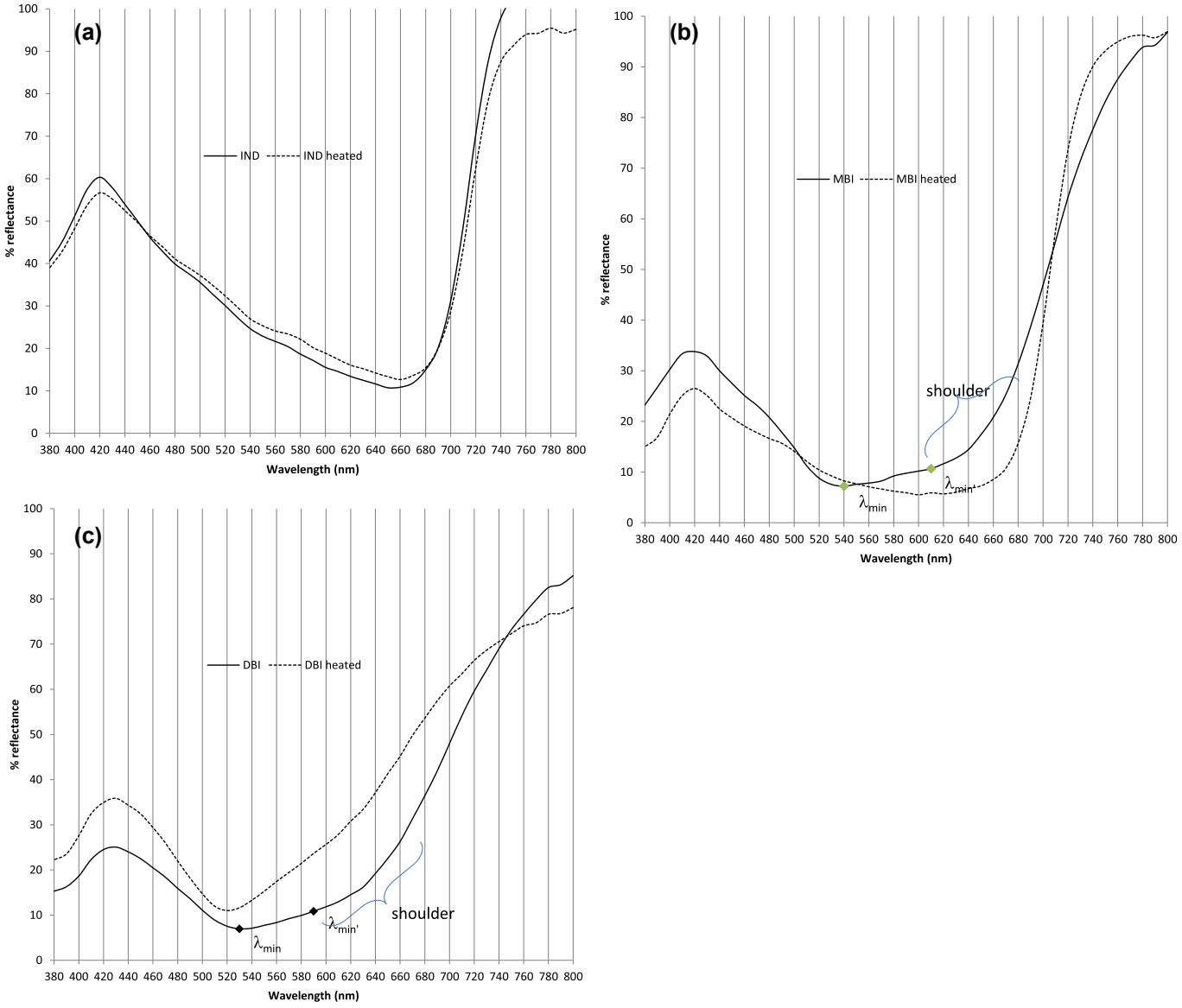

Fig. 2. Reflectance spectra of (a) indigo-, (b) MBI-, and (c) DBI-dyed wool, showing the thermochromic effect.

which gives a minimum at 533 nm and a broad shoulder in the blue-green region of the spectrum. That this shoulder is not due to indigo was proved by HPLC data, which showed no debromination had taken place after dyeing. Conspicuously absent in the spectrum of DBI-dyed wool from that study is a shoulder in the blue region. Based on this single reported absence of a "blue" shoulder in DBI-dyed wool, it was asserted [15] that wool dyed with DBI by others must contain MBI, which might have arisen from photo-debromination of the *leuco*-DBI. However, we have found that the reflectance spectrum of DBI-dyed wool shows the "blue" shoulder even when the vat is protected from light [10], and find that a shoulder on the minimum is almost always seen, regardless of fabric (see Table 2). Also, Cooksey and Sinclair have shown that even when the dye vat is not protected from ambient light, debromination does not occur on the time-scale of a dyeing experiment [9]. The anomalous spectral feature seen in Koren's DBI-dyed wool may arise from an inconsistent dyeing procedure. The dyed multi-fabric strips used in Koren's study were prepared by three of us (KR, OL, and SK) and used for analysis without our knowledge. We had discarded the method [13] used to prepare these samples in favor of a newer more reproducible method [9,10], because we found the older method to give variable colors and also led to unadsorbed dye particles on the surface of the fabric, especially in the case of DBI. Even more complicated is the case of a dyeing which contains all three indigoids. If a significant quantity of indigo is present, as was the case in wool dyed with Tyrian purple from a natural origin [19,20], then the reflectance spectrum can be highly misleading when used to characterize the components and their relative amounts in a sample.

3.2.2. Colorimetric analysis of dyed fabrics

To put the thermochromic effect on a quantitative basis, and also to make sure the apparent colors aren't deceiving the eye, CIELAB values were obtained for the multi-fabric strips from Fig. 1, before and after heating in water. Also, two three-pass dyeings – one of wool alone, the other of silk alone – were performed and analyzed for the thermochromic effect. In the CIELAB color space [21], a color is characterized by three attributes: the lightness, L^*, the hue, which

Table 2
Summary of first-pass reflectance data for 13 fabrics dyed with three indigoids each, and the directions of thermochromic effects.

fabric and treatment[a]		λ; min, shoulder (nm)[b] indigo	mbi	dbi	direction of spectral shift[c] indigo	mbi	dbi
acet.	cold	610, -	610, -	600, 520	blue	blue	red
	hot	660, -	610, 660	530, 590			
SEF	cold	610, 660	600, -[d]	600, 550	blue	blue	red
	hot	660, -	600, -[d]	530, 590			
triac.	cold	610, 670	600, -[d]	590, 530	blue	x	red
	hot	610, 690	600, -[d]	530, 590			
cott.	cold	660, -	610, 540[d]	540, 600	x	blue	red
	hot	660, -	600, -[d]	530, -			
cresl.	cold	610, 660	610, -	590, 540	blue	blue	red
	hot	650, -	610, -	530, 590			
dacr54	cold	610, -	610, -	600, 560	blue	x	x
	hot	610, 660	610, -	600, 560			
dacr64	cold	610, -	600, -[d]	600, -[d]	blue	x	x
	hot	610, 670	600, -[d]	600, 560[d]			
nylon	cold	620, -	(440-640)	610, 560	blue	x	red
	hot	660, -	(440-640)	530, 590			
orlon	cold	650, -	610, -	600, 550	x	x	red
	hot	650, -	610, -	530, 590			
silk	cold	630, -	610, -[d]	600, 540[d]	blue	x	red
	hot	660, -	600, -[d]	530, 590[d]			
polyp.	cold	660, -	530, 600	530, -	x	blue	x
	hot	660, -	(540-630)	530, 590			
rayon	cold	660, -	530, 600	530, 590	x	blue	x
	hot	660, -	620, -	530, 590			
wool	cold	660, -	540, 610	530, 590	x	blue	red
	hot	660, -	(580-650)	520, -			

[a]For full fabric names, see Figure 1. "Cold" indicates no post-dyeing heat treatment,"hot" indicates dyed fabrics were placed in boiling water for 10 minutes.
[b]A dash indicates that no shoulder was seen. Numbers in parentheses indicate a very broad peak.
[c] "Blue" indicates that a boiled fabric either showed a shift in its λ_{min} towards longer reflected wavelengths, or developed a shoulder at longer wavelengths, or that there was an exchange of positions between λ_{min} and a shoulder; "red" indicates these same kinds of changes toward shorter reflected wavelengths; an "x" indicates no thermochromic effect.
[d]Value taken from the corresponding second-pass dyeing; see text.

is given by two values, a^* and b^*, and the saturation, which is indicated by the absolute values of a^* and b^*. The L^* value varies from 0 (black) to 100 (white), while the a^* value is positive for redness and negative for greenness, and the b^* value is positive for yellowness and negative for blueness. High absolute values of a^* and b^* signify a highly saturated or vivid color, while low absolute values of these mean a color towards gray.

3.2.2.1. Wool- and silk-alone dyeings. Because wool and silk are the most historically significant fabrics, and they dye well with all indigoids, three-pass dyeings of each fabric with each dye were carried out, along with thermochromic studies of each pass. The data are shown graphically in Fig. 3, where the hue of each dyeing, unheated and heated, is represented by two bars. (Raw data with standard deviations, and the third-pass data, are given in Table S2 in the Supplementary Data section.) Production of the silk dyeings and their reflectance spectra are described in our preliminary report [10]. We now add colorimetric characterization of these dyeings. Also, three three-pass wool dyeings using the standard concentration of each dye were produced and characterized by colorimetry, for comparison to the silk dyeings. The ΔE_{ab}^* value [21] is a measure of the difference between two colors, and is the Euclidean distance between two points in the three-dimensional color space. The formula for ΔE_{ab}^* is the square root of the sum of

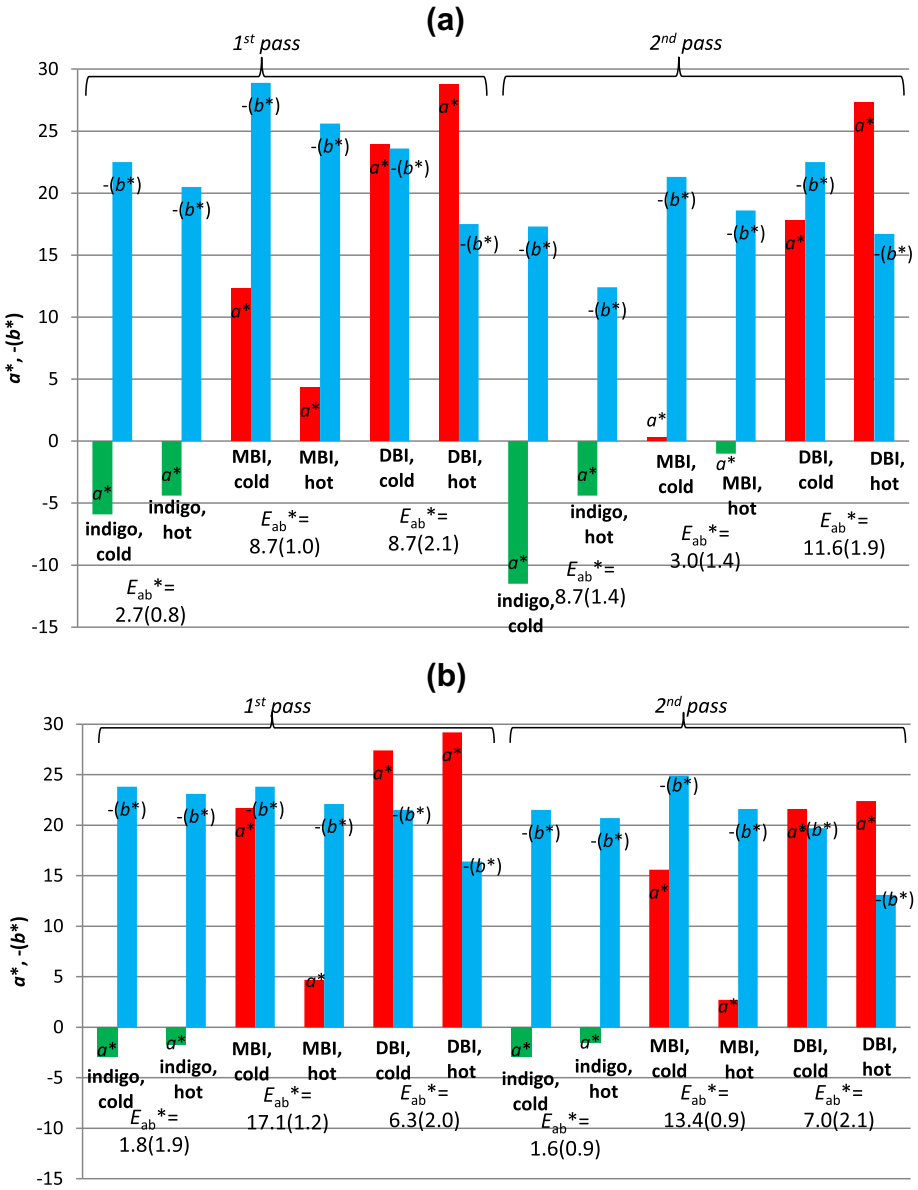

Fig. 3. CIELAB data from the first- and second-pass (a) silk dyeings and (b) wool dyeings. Color differences (ΔE_{ab}^*) are between the unheated fabrics (cold) and fabrics heated in boiling water for 10 min (hot). The standard deviations (in parentheses) were estimated by plugging into the color difference formula the highest and lowest values from the standard deviations of the L^*, a^*, and b^* values (see Table S2 in the Supplementary Data section).

the squares of the changes in L^*, a^*, and b^* values. Here, it measures the change in color before and after heating. We have found that a color change in these samples can be discerned for ΔE_{ab}^* values as low as four. In cases where the standard deviation roughly equals or is greater than ΔE_{ab}^*, this indicates the two samples exhibited no difference in color. Also, we found that changes in the L^* value upon heating were in most cases slight, so the color changes perceived are primarily due to changes in hue and saturation rather than lightness.

Heating of the indigo silk-alone dyeings resulted in partial loss of saturation in both color components, for all three passes. The thermochromic effect is expressed as a graying of the fabric upon heating.

In the MBI silk-alone dyeings, the colorimetric behavior upon dilution and heating is more complex. While the blue component diminishes in magnitude in a regular way, both upon dilution and heating, the a^* component changes from red to green upon dilution. In addition, the a^* component is partially leveled by heating (i.e. the heated values move towards or stay near zero). The result in all three cases is a bluing of the fabric, most evident in the first-pass dyeing which is the darkest and most highly saturated.

The DBI silk-alone dyeings show the greatest regularity in the change of colorimetric values, and the most evident color changes: Both red and blue components diminish regularly upon dilution, with red showing more diminishment; heating causes partial loss of the blue component in all three passes, while the red component is increased in all three passes. The result is a marked visible reddening of the fabrics for each pass upon heating, which is corroborated by the reflectance spectra that show lessening of shoulders at longer wavelengths for all three passes upon heating [10].

Fig. 3 also presents data for wool-alone dyeings. These show the same general trends as the silk dyeings, although to different degrees. The MBI dyeings show the greatest thermochromic effect,

Table 3
CIELAB data for the unheated and heated first-pass multi-fabric dyeings of Fig. 1.

fabric and treatment		indigo			MBI			DBI		
		L^*	a^*	b^*	L^*	a^*	b^*	L^*	a^*	b^*
acet.	cold	61.5	-2.1	-15.1	54.7	0.8	-5.3	56.5	5.7	-10.5
	hot	63.7	-1.2	-9.6	54.3	1.2	-4.3	58.8	11.5	-8.4
SEF	cold	72.6	-3.1	-8.8	55.3	0.5	-5.3	59.1	5.9	-11.6
	hot	71.6	-2.1	-7.3	56.9	0.5	-5.4	62.3	9.0	-7.6
triac.	cold	59.9	-0.4	-16.0	58.1	0.7	-4.4	60.1	5.6	-9.3
	hot	60.6	-1.2	-9.7	54.2	1.4	-4.3	61.6	8.8	-7.2
cott.	cold	71.4	-2.8	-9.3	68.4	2.3	-10.7	71.7	8.2	-10.0
	hot	71.9	-2.6	-9.5	69.8	0.2	-7.6	71.5	8.0	-7.3
cresl.	cold	78.8	-2.7	-6.4	71.1	-0.8	-10.6	74.6	3.9	-8.4
	hot	80.4	-1.2	-4.1	71.1	-0.1	-7.8	75.9	5.1	-5.4
dac54	cold	76.7	-4.1	-8.9	63.7	-0.7	-13.3	68.4	3.1	-11.5
	hot	78.3	-3.3	-7.0	63.4	-1.0	-11.6	69.7	3.0	-10.5
dac64	cold	68.1	-4.2	-13.8	55.1	1.3	-9.3	55.8	3.9	-10.4
	hot	67.6	-3.5	-11.4	55.0	1.4	-7.3	57.6	5.9	-8.2
nylon	cold	59.3	-3.6	-14.0	54.1	1.1	-3.7	54.3	3.4	-7.1
	hot	62.3	-1.4	-9.4	54.4	2.2	-3.3	56.7	6.4	-8.2
orlon	cold	79.3	-2.5	-5.7	71.1	-0.6	-10.6	72.1	4.7	-9.0
	hot	81.0	-1.5	-4.6	71.8	0.2	-8.1	74.2	7.1	-7.1
silk	cold	68.6	-5.3	-9.0	59.5	1.3	-13.1	62.0	7.7	-13.6
	hot	68.4	-2.3	-7.0	62.7	1.2	-10.2	63.8	12.6	-9.3
polyp.	cold	78.0	-2.9	-6.2	69.6	4.6	-8.1	67.0	9.5	-7.9
	hot	78.3	-2.5	-5.7	68.2	2.0	-8.5	69.6	8.4	-7.1
rayon	cold	69.9	-2.9	-9.5	68.0	5.2	-9.7	69.5	9.4	-8.5
	hot	69.3	-2.3	-9.7	69.6	-0.3	-8.1	73.0	9.4	-7.3
wool	cold	60.3	-2.0	-10.9	58.7	4.3	-7.7	56.9	7.7	-7.2
	hot	60.7	-2.1	-9.5	56.3	0.8	-7.2	56.9	8.8	-6.0

with substantial loss of the red component upon heating. This results in a marked bluing for each pass. On the other hand, DBI dyeings show marked loss of the blue component after heating, while the red component remains constant. Indigo dyeings show little or no thermochromicity at all concentrations.

3.2.2.2. Multi-fabric dyeings. The analysis of the multi-fabric strips was problematic, as the fixed aperture of the colorimeter used was too large for the small fabric pieces of the strip. Thus, a custom-made smaller aperture was fashioned as described in Section 2.2.3. The data for the unheated strips (Table 3) is consistent with that from a previous study [15]: All samples show a strong blue component (-b^*); for indigo, a^* is always a small negative number; for MBI, a^* is usually positive but sometimes near zero; for DBI, a^* is always a positive number, and larger than the corresponding values for MBI. Thus, the colorimetry data is consistent with the reflectance spectra, and corroborates the visual evidence: Indigo dyes blue-green to blue, MBI dyes blue to blue-violet, and DBI dyes blue-violet to purple (with purple being defined as a roughly even mixture of blue and red).

Heating of the dyed strips in water for 10 min causes slight variable changes in L^*values, while nearly all of the samples lose saturation in the blue component regardless of fabric or dye. The direction of the change in a^* values is more variable. For indigo, the a^* values become less negative, resulting in a weaker green component. Since both components become less saturated, the result is a graying of the fabric in some cases, and no perceptible change in others. For MBI, the changes in the red/green component are variable. For the unheated fabrics with a relatively large red component ($a^* > 2$), heating causes a significant loss of this, resulting in either a perceived blue color change – most notably for wool – or a graying of the fabric.

DBI shows the most obvious thermochromic effects on fabric. In the unheated DBI fabric samples, the red component plays a significant part in the hue of all fabrics, unlike most of the MBI fabrics. In some cases, it roughly equals the blue component (cotton and

Table 4
HPLC peak area comparison between dyes extracted from unheated and heated fabrics.

Dye and fabric		Area in micro-absorbance units × 10^{-4} (s.d.)[a]		% diff.
		Unheated	Heated	
MBI	Wool	3423 (373)	3095 (22)	10.1%
	Silk	5032 (221)	5144 (108)	2.2%
DBI	Wool	122.1 (10)	127.7 (18)	4.5%
	Silk	104.5 (16)	104.1 (15)	0.38%

[a] Average per mg of sample, from three analyses; standard deviation is in parentheses.

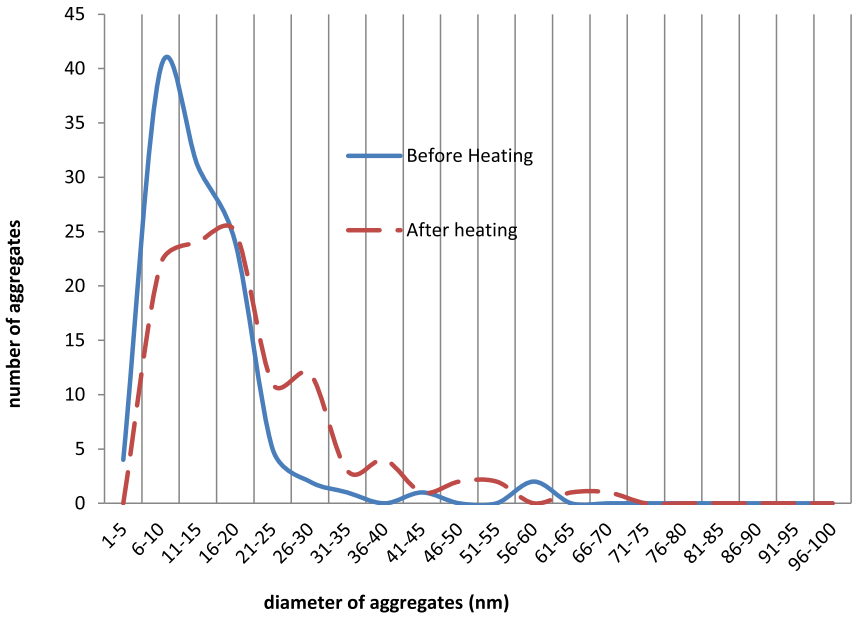

Fig. 4. Histogram of DBI-dyed nanotubes.

wool), or is even the dominant component (polypropylene and rayon). Almost all of the colors can be characterized as violets or purples of varying lightness. Heating of the DBI fabrics causes in all cases except nylon, a lessening of the blue component. This is accompanied by either a large gain in the red component, or virtually no change in some cases. Loss of blue and gain in red leads to an overall perceived reddening in seven of the thirteen fabrics, most markedly for silk.

Taking the indigo, MBI, and DBI multi-fabric dyeings together, the colorimetry data is mirrored by the reflectance data, which shows changes in the relative amounts of mainly two chromogenic species upon heating. In spite of widely varying fabric structures, almost all of the dyed fabrics show a heat-induced color change for at least one of the dyes. Thus, *the thermochromic effect is non-specific, showing slight or no dependence on the substrate the dye is applied to.*

3.3. HPLC analysis of extracts from unheated and heated dyed fabrics

To determine if the thermochromic effects are due in some way to chemical decomposition of the adsorbed dyes upon heating of the fabric, an HPLC study was undertaken. Four of the first-pass one-fabric dyeings were chosen for the analysis: MBI-dyed wool, MBI-dyed silk, DBI-dyed wool, and DBI-dyed silk. Small samples of each of these before and after heat treatment were extracted with DMSO, as described in Section 2.2.4., and the extracts were analyzed in triplicate by HPLC to check for loss of the dye. Table 4 shows the results. The relatively large standard deviations in some cases may be due to uneven dye loading. The low percent differences between the area counts before and after heat treatment are within the standard deviations and indicate no detectable chemical decomposition of the dye. *Thus, the thermochromic effect must be due to a physical change in the adsorbed dye.*

3.4. TEM analysis of dyed carbon nanotubes, and explanation of the thermochromic effect

As previously noted, some MBI-dyed fabrics turn more blue upon heating, while DBI-dyed fabrics turn more red. In our preliminary report [10], we proposed that the color change to blue upon heating of MBI-dyed fabrics is due to conversion of larger dye aggregates to smaller ones. This contention is based on changes in particle size seen after heating MBI-dyed carbon nanotubes. One would then predict that DBI-dyed nanotubes should show larger dye particles after heating, since MBI and DBI show opposite thermochromic effects on fabrics. We now show that this is the case.

TEM analysis was first applied to the dyed fabrics themselves, in an attempt to see the dye aggregates on fabric. But the fabric fibers were too large relative to the miniscule aggregates, so carbon nanotubes were envisioned as a fabric surrogate. We reasoned that, since the thermochromic effect is general for a wide variety of fabric molecular structures, the surface that the aggregates form on is not an important variable and hence the nanotubes are a valid surrogate for fabric. Thus, we vat-dyed carbon nanotubes with MBI and DBI in the same fashion as that used for the fabrics, and were gratified to see nanometrically sized dark (i.e. more electron-dense than carbon alone) dots on the surface of the dyed nanotubes in the TEM images (representative images can be found in the Supplementary Data section, in Figures S28 and S29). These were found to contain bromine by EDAX analysis, as described in the preliminary report [10], thus we characterize them as dye molecular aggregates. Unfortunately, this analysis did not allow us to see any physical features of the aggregates. Histograms of the aggregates were generated from the images, by size analysis of the dots, as described in Section 2.2.5. Fig. 4 shows the histogram for DBI-dyed nanotubes. Unheated dyed tubes show particles of mostly <10 nm in size; after heating in water for 10 min, most of the particles are significantly larger. Taken with the histogram of MBI-dyed nanotubes, which we revealed in the preliminary report [10] (see Figure S30 in the Supplementary Data section), it is strongly suggestive that changes in size of dye aggregates can account for the thermochromic effects and reflectance spectra of the dyed fabrics: For MBI, the initially large aggregates, which give rise to a reflectance λ_{min} around 530 nm, are diminished in size during heating in water. Thus, in the heated fabrics, the reflectance λ_{min} now appears in the blue region of the spectrum. For DBI, heating the fabric produces larger dye aggregates, resulting in, for example, loss of the “blue” shoulder in the reflectance spectrum of Fig. 2c.

It is well known that the aggregation state of dye and pigment molecules can affect their color. A classical case is the pigment cadmium sulfide, which can appear red or yellow irrespective of its polymorphic crystalline forms [22]. In dye chemistry, if the light absorption of an aggregate is red-shifted relative to the monomer, then the aggregate is of the J-type; if the aggregate's absorption is blue-shifted, then it is of the H-type [23,24]. If the analogy between aggregates in solution and on fabric (where the fabric plays the role of solvent) can be drawn, then the divergent thermochromic behavior of the brominated indigoids can be rationalized: MBI dye molecules on fabric form J-aggregates upon heating, appearing more blue, while DBI forms H-aggregates upon heating, appearing more red.

The dye aggregate sizes are ultimately determined by the number of bromine atoms the molecules contain. If single molecules of dye are considered, then the bromine atoms of MBI and DBI have only a small direct effect on the color of the molecules. This is evidenced by the very similar λ_{max} values of the three indigoids in their visible absorption spectra: 615 nm for indigo, 607 for MBI, and 598 for DBI, all in methanol solution [20]. The solutions are all shades of blue, and difficult to distinguish among, by eye. So the direct effect of a bromine atom is an eight-to nine-nm hypsochromic absorption shift (perceived color becomes nearly imperceptibly more red). However, the presence of bromine atoms in an indigoid has a profound effect on the aggregation state of the dyes when the molecules become attached to a fabric. Intermolecular forces of attraction between DBI molecules are enhanced due to van der Waals attractions between bromine atoms [13]. Thus, the brominated indigoids, relative to indigo itself, naturally form larger dye aggregates on fabrics, which appear successively more red as bromine atoms are added to the indigoid.

The thermochromic effect can be explained in the following way: When the *leuco* form of a brominated indigoid undergoes oxidation on a fabric, a metastable dye aggregate could be the result. In the case of MBI, the dye aggregate would be larger than normal; for DBI, the aggregate would be smaller than normal (with "normal" defined as thermodynamically more stable). The particle size of the dye and hence the color of the fabric would remain unchanged indefinitely, unless enough activation energy is supplied to allow conversion of the metastable aggregate to the more stable form. This energy can be supplied in the form of hot water, which causes MBI particles to form their more stable smaller type, and causes DBI particles to form their more stable larger type; the former is demonstrated by the histogram of Figure S30 in the Supplementary Data section, while the latter is demonstrated by the histogram of Fig. 4 in the text. Hence, the natural (defining "natural" as the most thermodynamically stable) color of MBI-dyed fabrics may be more blue, while that of DBI-dyed fabrics more red, than previously considered.

4. Conclusion

X-ray crystallographic data for MBI shows that the thermochromic behavior of a wide range of dyed textiles, which have not been subjected to any finishing procedures, is a property of the dye–textile combination rather than MBI itself. The spectacular difference between the colors of DBI dyeings, vs. the colors of MBI dyeings, on heating has been observed: DBI dyeings become more red while MBI dyeings become more blue. TEM studies suggest that the aggregation state of dye molecules is the major factor which contributes to the observed color of the dyeings. Although Pliny, who was writing from his armchair, does not mention the "improvement" of shellfish purple dyeings by boiling with water, it is possible that the effect was utilized in ancient times.

Acknowledgments

Testfabrics Inc. of Pittston, Pennsylvania, USA, is thanked for supplying the fabric strips used. Mr. Allen Ko, Mr. John Scalise, Mr. Derrick Claye and Ms. Aygul Islamova, all of Baruch College, CUNY, are thanked for experimental assistance. Ms. Jo Kirby of The National Gallery, and Mr. Greg Rohaus of Konica Minolta are thanked for helpful discussions. Dr. Frank Jacob of Queensborough Community College is thanked for translating articles from Japanese. OL thanks Anatoliy Lavinda for inspiring discussions. LM thanks Professor C. Michael Drain of Hunter College, CUNY, for suggesting use of TEM in this study and in reference 10, and for providing access to the microscope. The TEM instrument was purchased by funds from the RCMI programs G12 RR003037 and 8 G12 MD007599 from the National Institutes of Health. The Professional Staff Congress of the City University of New York is acknowledged for financial support of this work.

Appendix A. Supplementary data

Supplementary data related to this article can be found at http://dx.doi.org/10.1016/j.dyepig.2015.01.025.

References

[1] Jackson JW. The geographical distribution of the shell-purple industry. London: Longmans, Green and Co; 1917.
[2] Pliny the Elder. How wools are dyed with the juices of the purple. In: Historia Naturalis (The Natural History); 1st century AD, book 9, chapter 62.
[3] Kanold IB, Haubrichs R. Tyrian purple dyeing: an experimental approach with fresh Murex trunculus. In: Giner CA, editor. Purpureae vestes I. Textiles y tintes del Mediterráneo en época romana. València: Universitat de València; 2011. p. 253–6.
[4] Reinhold M. The history of purple as a status symbol in antiquity. Collect Latomus 1970;116:1–73.
[5] Schunck E. Notes on the purple of the ancients. 3. Purple dyeing in modern times. J Chem Soc 1880;37:613–7.
[6] Friedländer P. Über den Farbstoff des antiken Purpurs aus *Murex brandaris*. Ber Dtsch Chem Ges 1909;42:765–70.
[7] Koren ZC. Archaeo-chemical analysis of royal purple on a Darius I stone jar. Michrochim Acta 2008;162:381–92.
[8] Wouters J, Verhecken A. High-performance liquid chromatography of blue and purple indigoid natural dyes. J Soc Dye Colour 1991;107(7–8):266–9.
[9] Cooksey CJ, Sinclair RS. Colour variations in Tyrian purple dyeing. Dyes Hist Archaeol 2005;20:127–35.
[10] Lavinda O, Mironova I, Karimi S, Pozzi F, Samson J, Ajiki H, et al. Singular thermochromic effects in dyeings with indigo, 6-bromoindigo, and 6,6'-dibromoindigo. Dyes Pigments 2013;96:581–9.
[11] Karapanagiotis I, Mantzouris D, Cooksey C, Mubarak MS, Tsiamyrtzis P. An improved HPLC method coupled to PCA for the identification of Tyrian purple in archaeological and historical samples. Microchem J 2013;110:70–80.
[12] Tanoue Y, Terada A, Sakata K, Hashimoto M, Morishita SI, Hamada M, et al. A facile synthesis of Tyrian purple based on a biosynthetic pathway. Fish Sci 2001;67:726–9.
[13] Clark RJH, Cooksey CJ. Monobromoindigos: a new general synthesis, the characterization of all four isomers and an investigation into the purple colour of 6,6'-dibromoindigo. New J Chem 1999;23:323–8.
[14] Cooksey CJ. Making Tyrian purple. Dyes Hist Archaeol 1995;13:7–13.
[15] Koren ZC. Chromatographic and colorimetric characterizations of brominated indigoid dyeings. Dyes Pigments 2012;95:491–501.
[16] Szalda DJ, Ramig K, Lavinda O, Koren ZC, Massa L. 6-Bromoindigo dye. Acta Cryst 2012;C68:o160–3.
[17] Ziderman II, Wallert A, Hoffman R, Ozery Y. Bathochromic effect of heating 6-Bromoindigotin to 60 °C. In: 23rd dyes in history and archaeology Meeting, Montpellier; 2004.
[18] Ziderman II. The biblical dye *tekhelet* and its use in Jewish textiles. Dyes Hist Archaeol 2008;21:36–44.
[19] Koren ZC. The first optimal all-murex all-natural purple dyeing in the Eastern Mediterranean in a millennium and a half. Dyes Hist Archaeol 2005;20:136–49.

[20] Koren ZC. HPLC-PDA analysis of brominated indirubinoid, indigoid, and isatinoid dyes. In: Meijer L, Guyard N, Skaltsounis L, Eisenbrand G, editors. Indirubin, the red shade of indigo. Roscoff: Life in Progress Editions; 2006. p. 45–53.
[21] Schanda J. CIE colorimetry. In: Schanda J, editor. Colorimetry understanding the CIE system. Hoboken, New Jersey: John Wiley & Sons, Inc.; 2007. p. 58–64.
[22] Milligan WO. The color and crystal structure of precipitated cadmium sulfide. J Phys Chem 1934;38:797–800.
[23] Mishra A, Behera RK, Behera PK, Mishra BK, Behera GP. Cyanines during the 1990s: a review. Chem Rev 2000;100:1973–2011.
[24] Eisfeld A, Briggs JS. The J- and H-bands of organic dye aggregates. Chem Phys 2006;324:376–84.